

Synthesis and Characterization of Silver and Cobalt doped cobalt Ferrite by Glycine assisted sol-gel auto combustion method

Dr.G.Arumugam¹, Dr.R.Gopalakrishnan² Dr.S.Krishnaraj.³

S.M.Prabakaran.⁴

1. Assistant Professor of Physics ¹PG&Research Department of Physics, Annai Vailankanni Arts and Science College
Thanjavur-613007,
2. Associate Professor PSV College of Engineering & Technology. Krishnagiri.
3. Assistant Professor of Physics ³ Periyar Maniyammai University.Thanjavur.
4. Assistant Professor of Physics ³ Marudhupandiyar College Thanjavur .

Abstract:

The synthesized samples were characterized by X-ray diffraction (XRD), scanning electron microscopy (SEM), Fourier transform infrared spectroscopy (FTIR), UV-visible spectrum and vibrating sample magnetometer. The XRD and FTIR results confirm the formation of single phase cubic spinel structure of pure and Ag/Cd doped cobalt ferrite with fd3-m phase group. SEM analysis of surface morphology revealed that some spherical and cubic shaped cobalt ferrite nano particles. FTIR spectra indicated two fundamental absorption spectra around 582 cm^{-1} and 464 cm^{-1} . This confirmed the presence of metal-oxygen bonding in the synthesized samples corresponding to the vibrational stretching of both tetrahedral and octahedral lattice sites. From UV-Visible analysis it was observed that the optical band gap value varies from 1.52 eV to 1.88 eV as Ag/Cd concentration increased. From vibrating sample magnetometer data, the magnetic behaviour of the prepared samples were studied and the corresponding variations in the saturation magnetization (Ms), coercivity (Hc) and remnant magnetization (Mr) and squareness values were analyzed.

Keywords Silver Doped CoFe₂O₄; X-ray diffraction (XRD), scanning electron microscopy (SEM), Fourier transform infrared spectroscopy (FTIR), UV-visible spectrum and vibrating sample magnetometer.

Date of Submission: 29-01-2022

Date of Acceptance: 10-02-2022

I. Introduction

The spinel ferrite is one of the important ferrite group with general formula $M^{2+}Fe^{3+}_2O_4$ where M^{2+} is the divalent metal atoms such as Ni, Cd, Co, Cu, Mg and Mn etc., Spinel ferrite have numerous applications in catalysts, magnetic storage devices, sensors, optical devices, electronic devices for high frequency applications and magnetic refrigerators [1-5]. The silver doped cobalt ferrite nano particles shows their potential applications in biomedical fields such as magnetic guided drug delivery, magnetic resonance imaging and magnetic hyperthermia. Due to their unique characterizations such as moderate saturation magnetization, high magneto crystalline anisotropy, high electrical properties, good mechanical hardness and chemical stability, the cobalt ferrite with inverse spinel structure have become enormously popular among other magnetic materials [6-15]. It is known that the fascinating structural optical and magnetic properties of cobalt spinel ferrites depend on the nature of the ions and charge distributions. Generally, tetrahedral (A) sites occupied by Fe^{3+} ions, whereas octahedral (B) sites are inhabited by Co^{2+} and Fe^{3+} ions to alter structure and magnetic properties of nano particles[16-19]. It is necessary to modify their composition and microstructures by various synthesized routes.

In the present work, we report the synthesis of $Ag_xCd_xCo_{1-2x}Fe_2O_4$ (where $x=0.0, 0.05, 0.1$) nano particles by sol-gel auto combustion method using most famous and attractive fuel glycine. Glycine used for producing highly uniform complex oxide particles with precisely controlled stoichiometry. Mostly fuel is significant segment for the preparation of nano sized particles especially glycine. So far, several synthesis routes have been used for the preparation of ferrite nano particles such as, micro emulsion, co-precipitation, sol-gel, ball milling, hydrothermal flash method, electro-spinning and ceramic method [20-25]. Among them sol-gel

auto combustion method considered as much better for being short processing time, Low temperature, produces homogeneous particle of uniform size and low cost. This method results in the formation of pure phase $Ag_xCd_xCo_{1-2x}Fe_2O_4$ (where $x=0.0, 0.05, 0.1$) samples were characterized by means of x-ray diffraction (XRD). The Fourier Transform Infrared Spectroscopy (FTIR) were used to confirm the position of the ions in the synthesized samples, the chemical composition and morphology of the samples analysed using scanning electron microscopy (SEM). The optical and magnetic properties of the prepared samples were carried out by using UV-visible spectroscopy and vibrating samples magnetometer (VSM). In literature several studies have been reported with cadmium doped cobalt ferrite and silver doped cobalt ferrite separately. To author's knowledge, no investigation has been made on synthesis and characterization of Ag and Cd co-doped cobalt ferrite.

II. Experimental

Synthesis

Pure and Ag/Cd doped cobalt ferrite powders with chemical formula $Ag_xCd_xCo_{1-2x}Fe_2O_4$ (where $x=0.0, 0.05, 0.1$) were prepared by the glycine assisted sol-gel auto combustion technique. Analytical grade of purified cobalt nitrate $[Co(NO_3)_2] \cdot 6H_2O$, iron (III) nitrate, $Fe(NO_3)_3 \cdot 9H_2O$, silver nitrate $[Ag(NO_3)_2]$ Cadmium nitrate and citric acid (weighed as citric acid /metal ion mole ratio (1:1.5) were weighed and dissolved in stoichiometric amount of 50 ml of de-ionized water and stirred continuously using magnetic stirrer attached with hot plate. Dilute ammonia (NH_3) solution was dropwisly added to the mixed solution during constant stirring and pH of the resulting solution was adjusted 6-7. The appropriate amount of fuel (glycine) was added to the solution. The temperature of the hot plate was maintained at 60° for 5 hours. The water was slowly evaporated than the solution was kept at hot air-oven at 120° for 12 hours. The mixed solution gets changed from sol into gel and then the gel was completely dried. The agate mortar and pestle was used ground the dried samples into powder. The powder further annealed with muffle furnace at 800° for threehours.

Characterization

The structural and phase identification of prepared samples were characterized by powder x-ray diffraction method (Shimadzu XRD 600 x- ray diffractometer with $Cu\ \alpha$ radiation; $\lambda= 1.5406\text{\AA}$) operating at 40kv and 30m. The Fourier Transform-Infrared spectra were recorded using a Perkin-Elmer FT-IR spectrophotometer with KBr pellets. The surface morphology was analyzed by Scanning Electron Microscope (SEM- JSM-IT200). Saturation magnetization (M_s), remenant magnetization (M_r) and coercive magnetization (H_c) were found using the Vibrating Sample Magnetometer (VSM-Lake shore model 7404). The Optical properties have been studied by Perkin Elmer UV-Vis- NIR and spectrometer (Model: Lambda 35) in the range 190-1100nm.

III. Result and discussions

XRD analysis

The phase formation and crystalline nature of the synthesized samples were identified using x- ray diffractometry. Fig.1 shows the XRD pattern of the prepared pure and Ag/Cd doped cobalt ferrite samples.

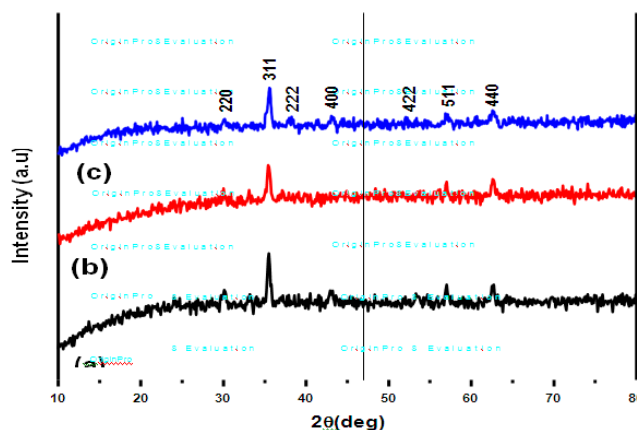


Fig.1. XRD pattern of $Ag_xCd_x Co_{1-2x}Fe_2O_4$ Spinel ferrites: (a) $X=0.0$, (b) $X=0.05$ and (c) $X=0.1$.

The Debye- Scherrer's equation were used to determine the particle size from most intense peak (311) [30-31]

$$D = \frac{0.9\lambda}{\beta \cos\theta} \quad \text{----- (1)}$$

Where the value 0.9 is shape factor, β is the full width half maximum, λ is the wavelength and θ is the diffraction angle.

The lattice parameter (a) value of spinel cobalt ferrite were calculated by using the equation [30]

$$a^2 = \frac{d^2}{(h^2+k^2+l^2)} \quad \text{----- (2)}$$

Where, d is interplanar distance, a is lattice constant and hkl are miller indices.

Table 1. XRD pattern of synthesized Ag_xCd_xCo_{1-2x}Fe₂O₄(where X=0.0, 0.05 and 0.1) spinel ferrite samples

Sample	2 Theta (deg)	Crystallite size (nm)	Lattice parameter (a) Å	Volume (Å) ³
CoFe ₂ O ₄	35.700	14.956	8.296	570.96
Ag _(0.05) Cd _(0.05) Co _(0.9) Fe ₂ O ₄	35.425	17.329	8.379	588.26
Ag _(0.1) Cd _(0.1) Co _(0.8) Fe ₂ O ₄	35.365	19.589	8.388	590.16

The lattice parameter (a), crystallite size (d) and reflection angles for most intense reflection peaks are listed in table 1. It is seen from the table that the lattice parameter was calculated as a=8.296Å, 8.379Å and 8.388Å respectively. The crystallite sizes are found to be 14.95 nm, 17.329 nm and 19.589 nm according to the maximum reflection peak (311) using Debye Scherer's relations.

It is clear from the table, the crystallite size (d) and lattice constant (a) was increased with increase Ag/Cd content attributed to the larger ionic radii of silver and cadmium ions (Ag: ionic radius 1.29Å and Cd: 1.038Å) enter into the spinel structure of cobalt (ionic radius of Co: 0.72Å and Fe: 0.67Å) ferrite and displace the cobalt ions and iron ions respectively. The unit cell volumes also increased due to the larger ionic radii of the dopant content into the smaller ionic radii ions. The intensity of the reflection peaks are decreased due to defect and disorder in Ag and Cd in the cobalt ferrite.

SEM analysis

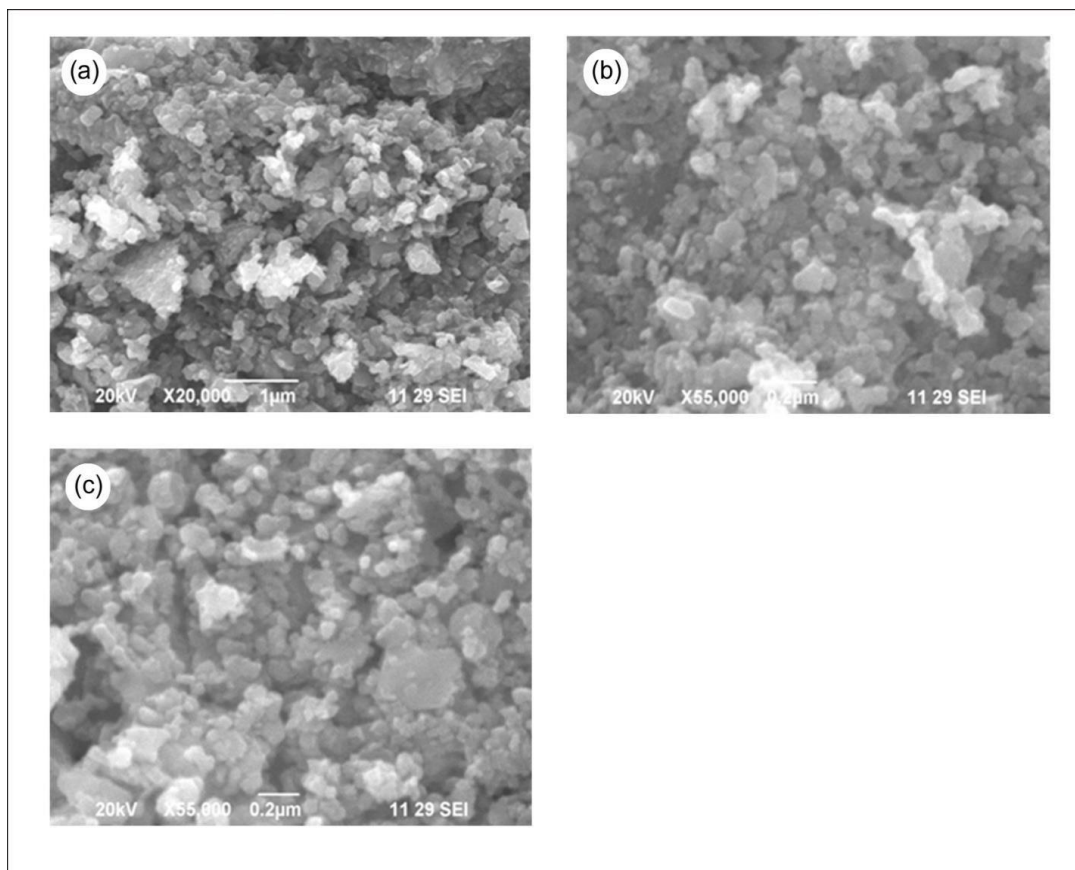


Fig.2. SEM images of synthesized $Ag_xCd_x Co_{1-2x}Fe_2O_4$ spinel ferrites: (a) $X=0.0$, (b) $X=0.05$ and (c) $X=0.1$.

The surface morphology of the prepared samples was analysed using scanning electron microscopy. SEM images of the samples $CoFe_2O_4$, $Ag_{0.5}Cd_{0.5}Co_{0.9}Fe_2O_4$ and $Ag_{0.1}Cd_{0.1}Co_{0.8}Fe_2O_4$ are shown in figure 2.(a), (b) and (c) respectively. All the images reveal that the samples exhibit a compact arrangement of uniform distribution of nanoparticles with a mixture of spherical and cubic shapes [31, 32]. For all the samples of pure and doped cobalt spinel ferrites, there was an increasing in particle size with increasing dopant content.

FTIR analysis

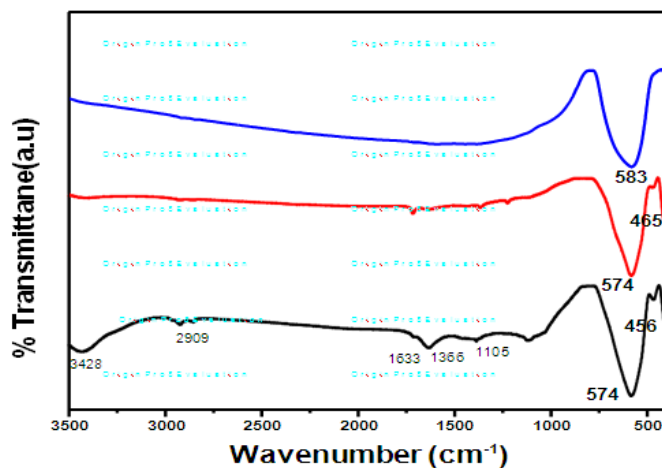


Fig.3. FTIR spectra of synthesized $Ag_xCd_x Co_{1-2x}Fe_2O_4$ spinel ferrites: (a) $X=0.0$, (b) $X=0.05$ and (c) $X=0.1$.

Fourier Transform Infrared spectroscopy gives significant information about position of the ions with respect the nature of functional groups present in the cobalt ferrite nanoparticles. Fig.3 shows the FTIR spectra of the synthesized samples at room temperature in the frequency range 400-4000cm⁻¹. The formation of single phase spinel structure (A²⁺B₂³⁺O₄) were observed in the absorption band frequency range 400-650cm⁻¹ attributed to the divalent and trivalentions distributed over A-site and B-site respectively. In present study we observed the lower frequency band (ν₁) at 456cm⁻¹ 465 cm⁻¹ attributed to the stretching vibrations of the octahedral group of metal-oxygen bond and the higher frequency bands (ν₂) at 574 cm⁻¹to 583 cm⁻¹ attributed to the stretching vibrations of the tetrahedral group of metal-oxygen bond. The vibrational frequencies of Infrared bands and of samples synthesized by sol-gel auto combustion method, which are good agreeing with previous researchers [33-35].

UV-Vis studies

The optical properties such as, band gap value and electronic spectra of the synthesized samples were characterized by UV-Visible spectrometer with 200-800 nm range. The UV absorption spectra of cobalt ferrite samples with various concentrations of Ag/Cd concentrations are shown in fig. 4. The absorption spectra of prepared cobalt ferrite samples exhibited in the visible region. The optical band gap energy value of the prepared cobalt ferrite sample was estimated using the relation [36]

$$(\alpha h\nu)^2 = B(h\nu - E_g) \quad (3)$$

Where B is a constant, h is the Plank’s constant and ν is the incident energy of radiation.

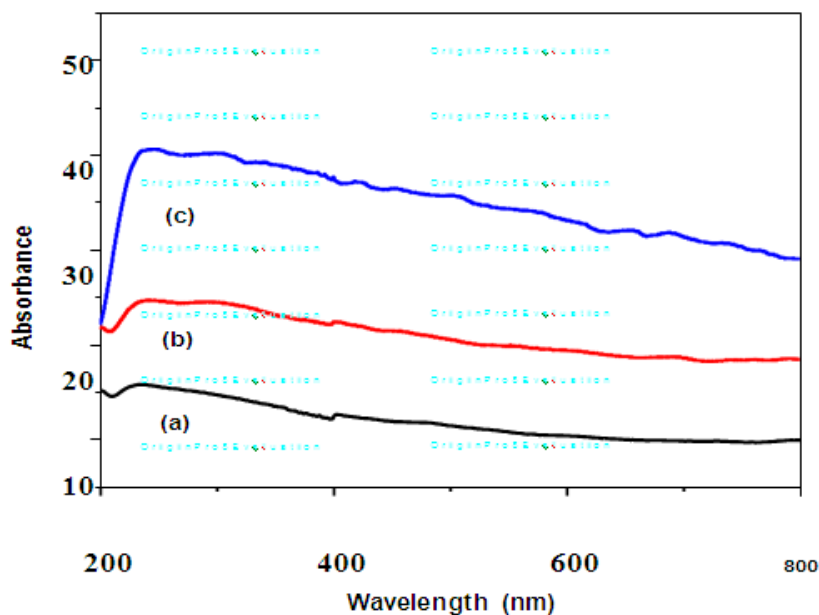


Fig.4. Optical absorption spectra of Ag_xCd_x Co_{1-2x}Fe₂O₄ spinel ferrites: (a) X=0.0, (b) X=0.05 and (c) X=0.1.

The optical band gap energy values have been evaluated by extrapolating the linear part of the graph of (αhν)² against E_g. The E_g values of the prepared samples are 1.88eV, 1.74eV and 1.52eV.

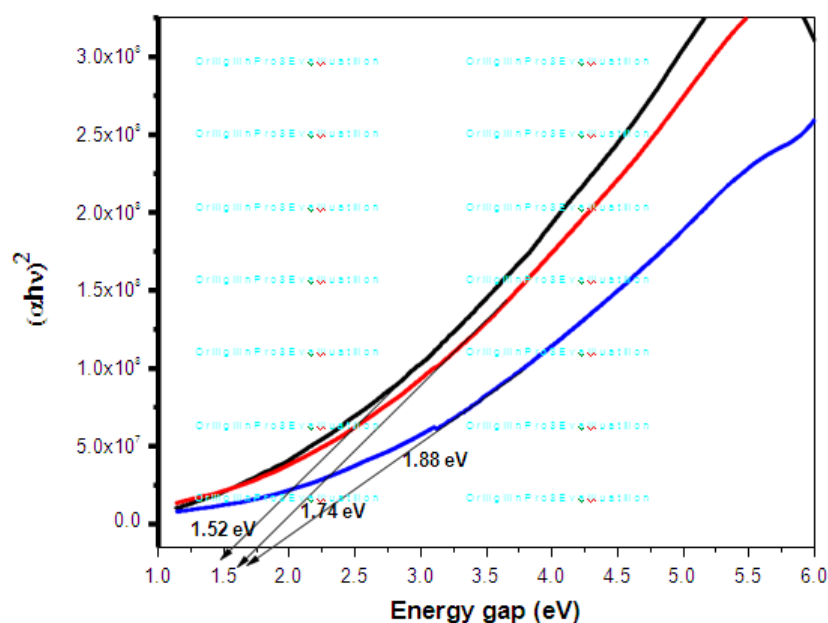


Fig.5. Optical band gap energy of $Ag_xCd_xCo_{1-2x}Fe_2O_4$ spinel ferrites: (a) $x=0.0$, (b) $x=0.05$ and (c) $x=0.1$.

The tauc plot of $(\alpha h\nu)^2$ vs $h\nu$ has been exhibited in fig.5 it is observed from the figure that the band gap energy values are decreases with Ag/Cd dopant concentration in cobalt ferrite increase. This may be attributed to the increase in defects, impurities, oxygen vacancies and weak quantum confinement effect respectively. The particle size and band gap energy values were varies as inverse proportion according to previous report [37-39]. The obtained band gap energy values from present study suitable for the role of solar light photocatalyst applications.

Magnetic studies

Magnetic behaviors of synthesized $Ag_xCd_xCo_{1-2x}Fe_2O_4$ (where $x=0.0, 0.05, 0.1$) nano particles were analysed by Vibrating sample magnetometer (VSM) at room temperature with an applied magnetic field 30000 Oe. The magnetic parameters such as saturation magnetization (M_s), remenant magnetisation (M_r), coercivity (H_c), Squareness value (M_r/M_s) and magneton number nB for the prepared samples with various concentrations were calculated and listed in table 2. M-H curves of Ag/Cd doped samples exhibit soft magnetic in nature as compared with cobalt ferrite, this was shown in fig.6. The magnetic properties of spinel ferrite depend on the various chemical composition, particle size and cationic distribution between octahedral and tetrahedral lattice sites. It was observed that, the saturation magnetization (M_s) values are 95.43, 89.90 and 73.51 emu/g. The remenant magnetization (M_r) values obtained from M-H loop were decreases as 49.67, 48.21 and 38.42. These analysis shows that the coercivity (H_c) of the prepared samples also decrease as 1228, 794 and 106 Oer respectively.

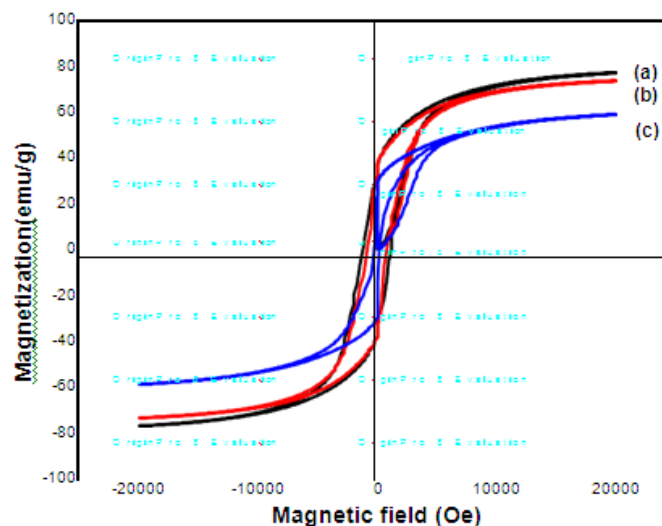


Fig.6. Hysteresis loops of $Ag_xCd_x Co_{1-2x}Fe_2O_4$ Spinel ferrites: (a) $X=0.0$, (b) $X=0.05$ and (c) $X=0.1$.

In spinel ferrite, the metal ions are located in two sub lattices namely, tetrahedral (A-site) and octahedral (B-site) arrangements. The magnetic moments are in opposite directions and they cancelled each other. The higher concentration of iron ion and cobalt magnetic ions at octahedral (B-site) site leads to enhance B-B exchange interaction and weakening of A-B interaction. These weakening interactions caused by substitution of non-magnetic Ag and Cd ions in the octahedral site and migration of Co ions to tetrahedral site, which lead to decrease the all magnetic parameters values [40-45].

The coercivity (H_c) value of the prepared samples depends on the magnetic crystalline anisotropy. In this study the coercivity is observed to decrease with increase non-magnetic behavior of Ag^{2+} and Cd^{2+} concentration attributed to decrease the magnetic crystalline anisotropy[40, 41]. The magneton number (n_B) was determined using the relation

$$n_B = (M_s \times M_w) / 5585$$

Where, M_s is saturation magnetization, M_w is molecular weight of the chemical composition. In pure cobalt ferrite the magneton number observed at $2.086 \mu_B$ and Ag/Cd doped cobalt ferrite it was observed that $2.1136 \mu_B$ and $1.647 \mu_B$. the squareness values (M_r/M_s) sharply increase as 0.52, 0.536 and 0.537 with increasing doping concentrations. This study confirms the M_s , M_r and H_c , values decreases with increasing doping concentrations may be attributed to non-magnetic nature and higher ionic radius of Ag and Cd dopant or may be due to exchanging A-B interactions.

IV. Conclusion

In this work Ag and Cd doped ferrite $Ag_xCd_xCo_{1-2x}Fe_2O_4$ (where $x=0.0, 0.05, 0.1$) were successfully synthesized by using glycine assisted sol-gel auto-combustion route. An XRD reflection peak confirms the cubic spinel crystal structure without any additional peaks. The average crystallite size found to be increased from 14.95 to 19.5 nm with an increasing in the dopant (Ag/Cd) concentrations. SEM images observed that all prepared samples have a mixer of spherical and cubic in shape. In FTIR spectra there was two absorption peaks observed near 460 cm^{-1} and 580 cm^{-1} confirm the spinel ferrite. UV- visible analysis confirms the absorption peaks of prepared cobalt ferrite samples exhibit in the visible region. The optical band gap energy values decreased from 1.88 eV to 1.52eV with increasing dopant concentrations. The magnetic properties such as: M_r , M_s and H_c decreases with increasing Ag and Cd concentrations. Saturation magnetization, remanant magnetization and coercivity values of Ag and Cd doped cobalt ferrite samples are very small compared to the pure cobalt ferrite which concluded that the nano particles are highly desirable candidate material for solar light photo-catalyst, high density data storing and bio- medical applications.

References;

- [1]. S. Alone, et al., Chemical synthesis, structural and magnetic properties of nano-structured Co–Zn–Fe–Cr ferrite, J. Alloys Compd. 509 (16) (2011)5055–5060.
- [2]. Zafar Q, Azmer M I, Al-Sehemi A G, Al-Assiri M S, Kalam A, Sulaiman K. Evaluation of humidity sensing properties of TMBHPET thin film embedded with spinel cobalt ferrite nanoparticles. J Nanopart Res 2016; 18:186.

- [3]. Alshehri S M, Alhabarah A N, Ahmed J, Naushad M, Ahmad T. An efficient and cost effective tri-functional electrocatalyst based on cobalt ferrite embedded nitrogen doped carbon. *J Colloid Interface Sci* 2018; 514:1.
- [4]. S. Munjal, et al., Water dispersible CoFe₂O₄ nanoparticles with improved colloidal stability for biomedical applications, *J. Magn. Magn Mater.* 404 (2016)166–169.
- [5]. Kim D H, Nikles D E, Jhonson D T, Brazel C S. Heat generation of aqueously dispersed CoFe₂O₄ nanoparticles as heating agents for magnetically activated drug delivery and hyperthermia. *J Magn Magn Mater* 2008; 320:2390.
- [6]. Jordan A, Scholz R, Wust P, Föhling H, Felix R (1999) Magnetic fluid hyperthermia (MFH): Cancer treatment with AC magnetic field induced excitation of biocompatible superparamagnetic nanoparticles *J Magn Magn Mater*,201:413.
- [7]. Wang Li. , Yan Y. , Wang M. ,a Yang H. , Zhou Z et. Al. (2016) An integrated nanoplatform for theranostics viamultifunctional core–shell ferrite nanocubes *J. Mater. Chem. B*, 4, 1908- 1914.
- [8]. M.W. Mushtaq, M. Imran, S. Bashir, F. Kanwal, L. Mitu (2016)Synthesis, structural and biological studies of cobalt ferrite nanoparticles . *Bulgarian Chemical Communications*, Volume 48, Number3 (pp. 565 – 570)2016.
- [9]. Sonal singhal, Sheenu jauhuar, Kailash chandra and Sandeep bansal, Spin canting phenomenon in cadmium doped cobalt ferrites, CoCdxFe_{2-x}O₄ (x = 0-0, 0-2, 0-4, 0-6, 0-8 and 1-0), synthesized using sol–gel auto combustion method *Bull. Mater. Sci.*, Vol. 36, No. 1, February 2013, pp.107–114.
- [10]. Maaz K, Mumtaz A, Hasanain S K, Ceylan A. Synthesis and magnetic properties of cobalt ferrite (CoFe₂O₄) nanoparticles prepared by wet chemical route. *J Magn Magn Mater* 2007; 308:289.
- [11]. M. Hossain, Study of the Magnetic and Transport Properties of Ytterbium Doped Co-zn Ferrites, *Khulna University of Engineering & Technology (KUET), Khulna, Bangladesh*,2018.
- [12]. M.B. Ali, et al., Effect of zinc concentration on the structural and magnetic properties of mixed Co–Zn ferrites nanoparticles synthesized by sol/gel method, *J. Magn. Magn Mater.* 398 (2016)20–25.
- [13]. S. Amiri, H. Shokrollahi, The role of cobalt ferrite magnetic nanoparticles in medical science, *Mater. Sci. Eng. C* 33 (2013)1–8.
- [14]. N. Sanpo, J. Wang, C. Berndt, Influence of chelating agents on the microstructure and antibacterial property of cobalt ferrite nanoparticles, *J. Australas. Ceram.Soc.* 49 (2013) 84–91.
- [15]. S. Xavier, H. Cleetus, P. Nimila, S. Thankachan, R. Sebastian, E.M. Mohammed,Structural and antibacterial properties of silver substituted cobalt ferrite nanoparticles,*Res. J. Pharmaceut. Biol. Chem. Sci.* 5 (2014)364–371.
- [16]. Yafet Y and Kittel C 1952 *Phys. Rev.* 87:239.
- [17]. A.Pradeep, P. Priyadharsini, G. Chandrasekaran, *J. Alloys Compd.* 509 (2011)3917–3923.
- [18]. E. Prince, R.G. Srivastava, N.G. Navadikar, *Phys. Rev. B* 14 (1976)2032.
- [19]. Kanagesan S, Hashim M, Tamilselvan S, Alitheen NB, Ismail I, Syazwan M, Zuikimi MMM (2013) Sol-gel auto-combustion synthesis of cobalt ferrite and its cytotoxicity properties. *J. Nanomater Biostruct*8(4):1601–1610.
- [20]. Al-Shihri A S, Kalam A, Al-Sehemi A G, Du G, Ahmad T. One pot synthesis of Cobalt Ferrites nanoparticles via hydrothermal method and their optical studies. *J Indian Chem Soc* 2014; 91:1861.
- [21]. Mattei Y C, Pérez O P, Uwakweh O N C. Effect of high-energy ball milling time on structural and magnetic properties of nanocrystalline cobalt ferrite powders. *J Magn Magn Mater* 2013; 341:17.
- [22]. Malik H, Mahmood A, Mahmood K, Lodhi M Y, Warsi M F, Shakir I, Wahab H, Asghar M, Khan M A. Influence of cobalt substitution on the magnetic properties of zinc nanocrystals synthesized via micro-emulsion route. *Ceram Int* 2014; 40:9439.
- [23]. Yuksel Koseoglu, Furkan Alan, Muhammed Tan, Resul Yilgin, Mustafa Ozturk, Low temperature hydrothermal synthesis and characterization of Mn doped cobalt ferrite nanoparticles, *Ceram.Int*, 2012.*J.ceramint*.2012.01.001.
- [24]. Reddy, C. V., Byon, C., Narendra, B., Baskar, D., Srinivas, G., Shim, J., & Vattikuti, S. P. Investigation of structural, thermal and magnetic properties of cadmium substituted cobalt ferrite nanoparticles, *Superlattice Micros.* 82 (2015)165-173.
- [25]. M.M. Naik, et al., Green synthesis of zinc doped cobalt ferrite nanoparticles: structural, optical, photocatalytic and antibacterial studies, *Nano-Structures & Nano-Objects* 19 (2019)100322.
- [26]. A.Amri, et al., Developments in the synthesis of flat plate solar selective absorber materials via sol–gel methods: a review, *Renew. Sustain. Energy Rev.* 36 (2014)316–328.
- [27]. Sanpo N, Berndt CC, Wen C, Wang J (2013) Transition metalsubstituted cobalt ferrite nanoparticles for biomedical applications. *Acta Biomater*9(3):5830–5837.
- [28]. Patil SA, Mahajan VC, Ghatage AK, Lotke SD (1998) Structure and magnetic properties of Cd and Ti/Si substituted cobalt ferrites. *Mater Chem Phys*57(1):86–91
- [29]. H. Yan, et al., Influences of different synthesis conditions on properties of Fe₃O₄ nanoparticles, *Mater. Chem. Phys.* 113 (1) (2009)46–52.
- [30]. George M, Nair S S, John A M, Joy P A, Anantharaman M R. Structural, magnetic and electrical properties of the sol–gel prepared Li_{0.5}Fe_{2.5}O₄ fine particles. *J Phys D: Appl Phys* 2006; 39:900.
- [31]. M. O’Donnell, et al., Structural analysis of a series of strontium-substituted apatites, *Acta Biomater.* 4 (5) (2008)1455–1464.
- [32]. Ahmed HM (2015) Structural, electric and dielectric properties of cadmium doped nickel- cobalt ferrite *J Am Sci*11(8):69–72
- [33]. M. Ghariabshahian, M. S. Nourbakhsh, O. Mirzaee Evaluation of the superparamagnetic and biological properties of microwave assisted synthesized Zn & Cd doped CoFe₂O₄ nanoparticles via Pechini sol–gel method *Journal of Sol-Gel Science and Technology* <https://doi.org/10.1007/s10971-017-4570-1>
- [34]. B.Divya, B. Suman, M. Venkataswamy, K. Thyagaraju, A study on phytochemicals, functional groups and mineral composition of allium sativum (garlic) cloves, *Int. J.Curr. Pharmaceut. Res.* 9 (2017)42–45.
- [35]. Samavati A, Ismail AF (2017) Antibacterial properties of coppersubstituted cobalt ferrite nanoparticles synthesized by coprecipitation method. *Particuology*30:158–163
- [36]. A.M. Sertkol, Y. Koseoglu, A. Baykalb, H. Kavasa, A. Bozkurtb and M. S. Toprakc, *J. Alloys Compd.*, 2009, 486,325–329.
- [37]. V. Gupta, A. Mansingh, Influence of postdeposition annealing on the structural and optical properties of sputtered zinc oxide film, *J. Appl. Phys.* 80 (2) (1996)1063–1073.
- [38]. Kiran V S, Sumathi S. Comparison of catalytic activity of bismuth substituted cobalt ferrite nanoparticles synthesized by combustion and co-precipitation method. *J Magn Magn Mater* 2017; 421:113.
- [39]. S. Agrawal, A. Parveen, A. Azam, Structural, electrical, and optomagnetic tweaking of Zn doped CoFe₂ xZnxO₄ δ nanoparticles, *J. Magn. Magn Mater.* 414 (2016)144–152.
- [40]. J. Silama, et al., Magnetic properties of selected substituted spinel ferrites, *J. Magn. Magn Mater.* 326 (2013)251–256.
- [41]. I.Sharifi, H. Shokrollahi, S. Amiri, Ferrite-based magnetic nano fluids used in hyperthermia applications, *J. Magn. Magn Mater.* 324 (6) (2012)903–915.